POLITECNICO DI TORINO
Repository ISTITUZIONALE

Mechanical characterization and separation tests of a thermoplastic reinforced adhesive used for automotive applications

(Article begins on next page)

19 April 2024

AIAS 2019 International Conference on Stress Analysis

Mechanical characterization and separation tests of a thermoplastic reinforced adhesive used for automotive applications

Raffaele Ciardiello[a]*

*a*Politecnico di Torino, Corso Duca degli Abbruzzi 24, Turin 10129, Italy

Abstract

In the last decades, the use of structural and no structural adhesive has been increasing a lot in the automotive sector due to the advantages they can offer compared to traditional fasteners. Although they present many advantages, the impossibility to dismantle easily adhesive joints in order to substitute, recycle, reuse vehicle components or avoid waste for bonding errors is a factor that can limit their use. Furthermore, in Europe, the need to separate vehicle components for reuse and recycling is constrained by two Directives, 2000/53/EC and 2000/64/EC. These Directives set the objectives of reuse and recyclability for automotive vehicles, which are 95% and 85% respectively by an average weight per vehicle. For these reasons, it is very important to find a feasible solution to these problems. A promising technology for the separation of plastic joints, bonded with thermoplastic adhesives, uses nanomodified thermoplastic adhesives that are sensitive to electromagnetic fields. In this work, the mechanical behavior of adhesive joints made with a polyolefin adhesive, used in the automotive industry for bonding plastic components, have been studied. In particular, the adhesive has been modified with three different weight concentrations (3%, 5% and 10%) of iron oxide nanoparticles in order to make it sensitive to electromagnetic fields. These nanoparticles heat when are under the effect of an electromagnetic field and consequently they can melt the thermoplastic adhesive allowing for the joint separation. The mechanical properties of the joints prepared with the pristine and nanomodified particles have been studied by means of SLJ specimen with different overlap length and thicknesses. The adhesive joints prepared with the modified adhesives present a slightly higher load and a larger ductility compared to the ones prepared with the pristine one. Furthermore, separation tests have been performed in order to assess the times to disassemble these adhesive joints. Scanning electron microscope analysis has been used to assess the dispersion of the particles.

* Raffaele Ciardiello. Tel.: +39-011-090-6913; fax: +39-011-090-6999.
  E-mail address: raffaele.ciardiello@polito.it

1. Introduction

In recent years, the automotive industry is facing different challenges related to the weight reduction of the vehicles. On one hand, there is the strengthening of the environmental and safety regulations that suggest decreasing the weight of the vehicles by using lighter and more efficient materials. On the other hand, there is the increasing customer demand for higher performances and more luxury and safety features with a consequent weight addition. In this contest, adhesive bonding acquires great importance since it represents a lighter and cheaper solution, see Chang et al. (1999), Belingardi and Chiandussi (2004), Rudawska (2010) and Rudawska et al. (2019), in some cases, with respect to traditional fasteners. Adhesives permit to join component made of materials that are difficult or even impossible to join in other ways and they are able to join substrates made of different materials, such as composite materials with metals, see Belingardi et al. (2016) and Casalegno et al. (2018).

Although they offer some advantages, they cannot be easily separated. Lu et al. (2014) and Banea et al. (2013) reported some of the most traditional methods to separate adhesives joints such as: using chemical solvents, mechanical cutting or heat treatment. The use of heat and chemicals could damage the components (or substrates) because they can be aggressive not only for the adhesive but for the components as well. In this specific case, these techniques cannot be used for the reuse but only for recycling. Mechanical cutting is also complicated and it cannot be applied to many applications because, usually, the bondline of automotive components is included in the inner part of the components that have to be bonded. However, even though these techniques can work, in some case, it is very complicated to have a very clean surface in the bonding area of the adherends and they cannot be re-bonded easily. For this reason, most parts of the bonded components in automotive industries need a very complex procedure in order to be dismantled. Lu et al. (2014) and Banea et al. (2013) reported also many complex methods and new technologies that could separate mechanical adhesive joints but, even in this case, the surface of the adherends are not clean.

The possibility to dismantle components in the automotive industry is very important. In Europe, particularly, the Directive 2000/53/EC (2000), even called end-of-life vehicles (ELV) Directive and the Directive 2005/64/EC (2005) have set targets aiming the increase of the reusability, recoverability and recyclability of vehicle materials and components. Because of these directives, automotive industries must produce a detailed report for each model that show the existing techniques that they can use to dismantle components in order to recycle, reuse or recover those components. Automotive industries are required to achieve the recyclability of materials and components to a minimum of 85% by an average weight per vehicle and the reuse and recovery of components to a minimum of 95%. In this scenario, the development of disassembling technologies is crucial to reach the percentages of recyclability and reuse set by the directive. These Directives encourage automotive companies to find new approaches for the reuse and recycling of automotive vehicles before the adoption of new materials.

In the last decades, innovative technologies have been introduced and studied in automotive industries and research centers to find a feasible solution to these problems, see Banea (2019). Verna et al. (2013), Banea et al. (2015) and Ciardiello et al. (2018) have presented a technology that uses electromagnetic induction systems that activates magneto-sensitive nanoparticles embedded in adhesives. The sensitivity of these particles to the electromagnetic field has been used by Verna et al. (2013), Ciardiello et al. (2017) and Vattathurvalappil and Haq (2019) for rapidly increasing the temperature of thermoplastic adhesive allowing for the separation of joints with greater easiness and without damages. Banea et al. (2015) have used the same technology to heat metallic substrate in order to increase, by conduction, the temperature of thermally expandable particles. These particles are able to reduce the resistance section of the adhesive allowing for a separation of the joints. Severijns et al. (2018) have used the same technology for curing epoxy adhesives.

In electromagnetic induction process, an inductor is used to increase the temperature of a workpiece, usually a metallic component. Inductor works as a primary of an electric transformer and the conductive material as a secondary one. The electromagnetic field is generated by a coil that is the final element of the inductor and gives also the the shape of the electromagnetic. The temperature increase of the particles, in the case of iron oxide nanoparticles, is mainly due to the hysteresis losses and the Neel and Brown relaxation phenomena, see, Moskowitz et al. (1997), Bayerl et al. (2014), Suwanwatana et al. (2006). It is strictly linked to the dimension of the nanoparticles, in fact,

particles with a size smaller than 50 nm exhibit superparamagnetic behavior that leads to a more rapid increase of the temperature, as Ghazanfari et al. (2016) have reported.

As shown by Ciardiello et al. (2016), this is a promising technology to separate adhesive joints when nanomagnetite particles (Fe_3O_4) are embedded with hot-melt adhesives and coupled with electromagnetic induction systems. Although the separation times are short and can meet the industry requirements the mechanical properties need to be investigated because the introduction of particles in an adhesive matrix can lead to a reduction of the mechanical properties. In this work, the mechanical behavior of a polyolefin thermoplastic adhesive has been studied with a single lap joint. Three different adhesive thicknesses and six overlaps have been investigated on the pristine adhesive and on the same adhesive modified with 10% wt. The effect of the overlap and adhesive thicknesses have been studied only for the single lap joints prepared with the pristine HMA and HMA_10% since they showed a relatively significant difference compared to HMA_3% and HMA_5%. Furthermore, the effect of three weight percentages on the single lap joint test (3%, 5% and 10% wt.) was evaluated at a fixed overlap and thickness. The separation tests carried out with an electromagnetic induction system are presented for all the SLJ configuration. Visual inspection of the fractured SLJ specimens was presented as well together with the scanning electron microscope (SEM) analysis.

Nomenclature	
HMA	Adhesive joints prepared with the pristine hot-melt adhesive
HMA_3%	Adhesive joints prepared with the hot-melt adhesive modified with 3% wt. of iron oxide particles
HMA_5%	Adhesive joints prepared with the hot-melt adhesive modified with 5% wt. of iron oxide particles
HMA_10%	Adhesive joints prepared with the hot-melt adhesive modified with 10% wt. of iron oxide particles

2. Materials and methods

Mechanical tests were carried out on Single Lap Joint (SLJ) specimens prepared with three different adhesive thicknesses (0.5, 1.0 and 1.5 mm) and 6 overlaps (12, 18.5, 25, 31.5, 37 and 50 mm). On the other hand, separation tests were carried out only on three adhesive thicknesses (0.5, 1.0 and 1.5 mm) and three overlaps (12, 18.5, 25 mm) that are the specimen where a cohesive separation was observed in the mechanical tests. The adhesive thicknesses where chosen based on the analysis of a low tailgate used in the automotive industry and bonded with the hot-melt adhesive used in this work. The mean thickness is close to 1 mm but there are also some parts where the adhesive thicknesses reaches 0.5 and 1.5 mm. The mechanical properties of this adhesive at a fixed overlap and thickness were already studied in Ciardiello et al. (2018) together with the effect of the environmental conditioning of the joints prepared with the pristine and nanomodified adhesives. Furthermore, Ciardiello et al. (2017) and Ciardiello et al. (2018) studied the mechanical properties of this adhesive under dynamic conditions.

The joints used for the experimental tests were obtained by bonding substrates made of a polypropylene copolymer with 10% in weight of talc (Hifax CB 1160 G1, by Lyondell-Basell Industries). The substrates used in this work are 100 mm long, with a cross-section of 20 mm x 3mm. These substrates were bonded with a polyolefin-based HMA (Prodas, by Beardow Adams) a copolymer of polypropylene and polyethylene. The nanomodified adhesives were prepared by using a hot plate for melting the pristine adhesive and by adding iron oxide particles with an average size smaller than 50 nm (Fe_3O_4, by Sigma-Aldrich) with three different weight concentrations (namely 3%, 5% and 10%). This mixing procedure has been widely used in literature by Verna et al. (2018), Ciardiello et al. (2018) and Koricho et al. (2016). The particles have been chosen because nanomagnetite with a particles size smaller than 50 nm exhibit superparamagnetic behavior. Mechanical, thermal and chemical characterization of this pristine adhesive coupled with PP substrates can be found in Koricho et al. (2016). The characteristic values that are interesting for this work are the temperature at which this adhesive starts to degrade, that is 210 °C, the melting temperature that starts at 124 °C and ends at 150 °C, the open time that is 30 s and the density that is 0.98 g/cm^3.

Tensile tests were carried out on the substrate at 100 mm/min, which is the same speed adopted for the SLJ tests. This rate was chosen according to the Fiat Chrysler Automobile (FCA) standard on hot melt adhesive reported in Verna et al. (2018), Ciardiello et al. (2018) and Koricho et al. (2016). The mechanical tests were conducted using an

Instron 8801. Two tabs were bonded to the extremities to avoid the misalignment of the SLJ specimen. The main properties of the substrates are reported in Table 1.

Table 1. Mechanical properties of the substrates

Initial yield [MPa]	Max. tensile stress [MPa]	E [GPa]	$v_{elastic}$
15.1	20	1.90	0.4

Each substrate was cleaned with isopropyl alcohol in order to remove possible residuals from the specimen before the joints preparation. This is the procedure adopted by automotive industries to bond this adhesive. The joint preparation was performed with a hot-melt gun and an assembly device which permits the regulation of the adhesive thickness joint, as reported by Verna et al. (2018), Ciardiello et al. (2018) and Koricho et al. (2016). The thickness and the overlap of each joint were measured and it was found to be constant along the joint length, with a variation smaller than 0.03 mm.

Separation tests have been carried out to rate the speed of the dismounting process. The analysis has been conducted by using an electromagnetic inductor. The inductor used for this analysis was Heasyheat by Ambrell, with a maximum power of 10 kW and a frequency range from 10 to 400 kHz. The value of the current, frequency and the shape of the magnetic field have been chosen based on the outcomes of the work done by Ciardiello et al. (2019) in order to minimize the separation time. In this specific case, a power of 5.9 kW and a frequency of 317 kHz were used. For each test, a weight of 0.5 N was applied to the lower substrate of the SLJ in order to submit the joint to a constant load and cause joint separation (by part sliding) when the adhesive reaches its melting temperature. The separation process is shown in Figure 1 where the SLJ specimen is inserted inside the solenoid coil. These images have been recorded with an IR camera. Figure 1 (a) displays the start of the heating process, in fact, the temperature of the modified adhesive start to heat while the adherend temperature is low. Figure 1 (b) shows the sliding phase of the lower adherend that is connected to the 0.5 N weight. In this case, the adhesive is melted and the lower substrate is sliding. It is noticeable that part of the heat generated by the particles has been also transmitted to the adherend. Five replications have been carried out for the assessment of both mechanical and separation tests.
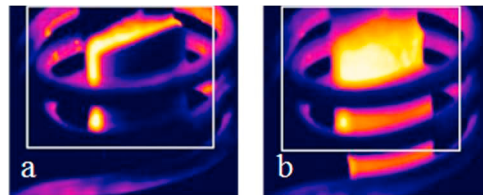

Fig. 1. (a) Initial phase of the heating process; (b) final sliding.

Scanning electron microscope (SEM) analysis was carried out using a Carl-Zeiss EVO50. An electronic high tension of 20 kV was used together with secondary emission signal. The specimens were properly coated with gold in order to have better images.

3. Results and discussion

3.1. Single Lap joint tests

Figure 2 shows the typical load-displacement curves of SLJ tests for the four adopted adhesive formulations, namely HMA_3%, HMA_5% and HMA_10% for an overlap of 25 mm and an adhesive thickness of 1 mm. The adhesive joint prepared with the pristine HMA is represented by the blue curve that is the lowest curve in the diagram. As illustrated, the increase of the particles weight content leads to an increase of the adhesive maximum loads and to a more ductile behavior of the modified HMAs, as can be noted by the larger tails on the right part. Representative curves of the SLJs prepared with HMA_3% and HMA_5% show that the values are almost superimposed in these two cases. The initial trends of the curves are equal for all the adhesive compositions. The increase of the maximum loads of the nanomodified adhesives could be due to the micro agglomerates that have been shown in the previous section.

These agglomerates lead to a toughening of the bondline that resulted in an increase of the maximum load and shear strength.
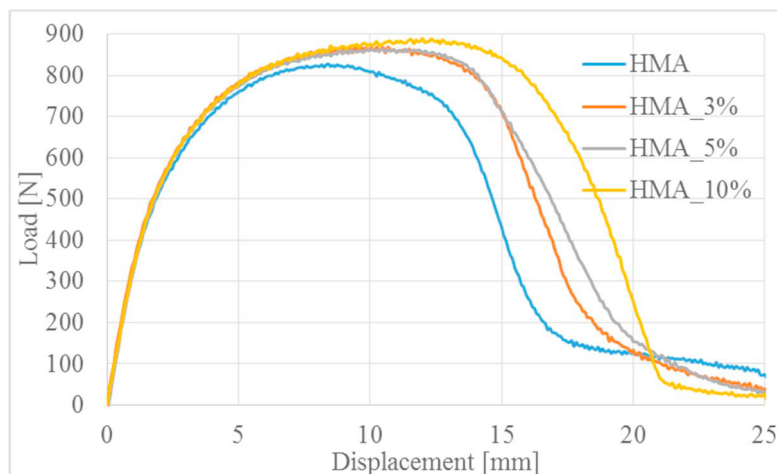

Fig. 2. Representative curves of SLJ tests for the three different adhesive compositions

Table 2 reports the maximum mean loads and shear strength calculated on the five replications for the case for the adhesive overlap of 25 mm and thickness of 1 mm. This Table illustrates that there is a percentage increase of 5.1%, 5.5% and 7.2% over the pristine adhesive for HMA_3%, HMA_5% and HMA_10% respectively. The standard deviations are very similar.

Table 2: Summary of the maximum adhesive shear strength

	Pristine HMA	*HMA_3%*	*HMA_5%*	*HMA_10%*
Average maximum load [N]	835.55	878.15	881.45	895.14
Average shear strength [N]	1.67	1.76	1.76	1.79
Standard Deviation [N]	22.52	20.27	30.84	16.66
Percentage increase [%]	– –	5.10	5.50	7.20

All the fracture surfaces of the SLJ specimens were evaluated after the test by means of visual inspection. Figure 3 (a) shows the three typical failures of adhesive joints. The first representation illustrates the cohesive failure, where the failure occurs within the adhesive layer. The second representative failure is called adhesive failure and it presents a complete separation between the adhesive layer and the substrate. Finally, substrate failure is shown.

As shown also by Koricho et al. (2016), the typical adhesive failure of these adhesive with polypropylene substrates or components is both cohesive and adhesive. This failure surface was obtained also by Ciardiello et al. (2017) in which a degrease process that uses sandpaper was used. Even in this work, the fracture surfaces present both cohesive and adhesive areas. In particular, the area very close to the edge presents an adhesive failure while the inner part is cohesive. This is particularly evident in Figure 3 (b) that shows a representative fracture surface a SLJ prepared with HMA_5%. The red lines illustrate the zones where the fracture was adhesive. In the remaining part, the separation was cohesive.

Figure 3 (c) displays representative fracture surfaces of the joints prepared with HMA, HMA_3%, HMA_5% and HMA_10% at a fixed thickness and overlap, respectively 1 and 25 mm. The cohesive zones are recognizable by the colors that are slightly clearer when compared to the zones where the separation was adhesive. Figure 3 (c) illustrates

that the introduction of nanoparticles increases the size of the cohesive fracture zone and it is worth to note that the size of cohesive fracture areas increases with the particle weight concentration.
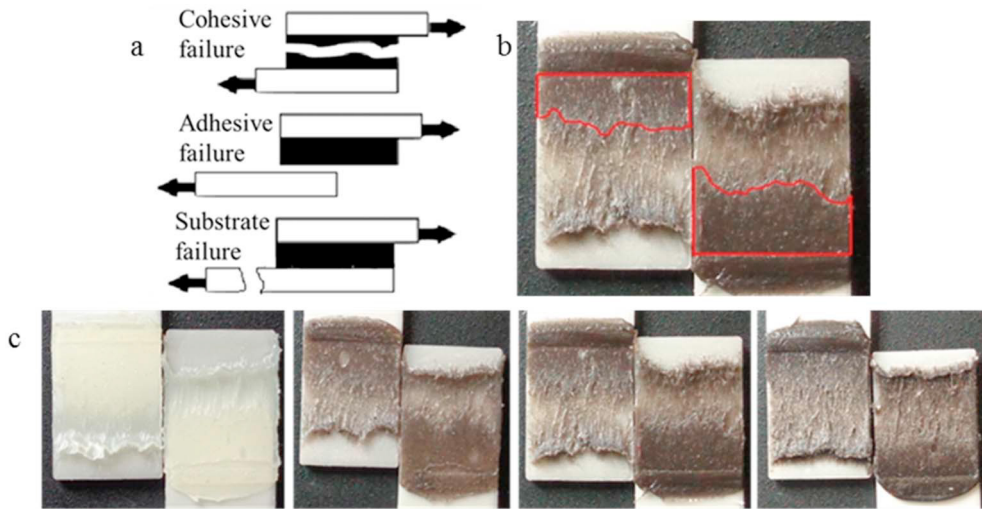

Fig. 3: (a) Representations of SLJ failure modes; (b) fracture surface of HMA_5%; (c) representative fracture surfaces of HMA, HMA_3%, HMA_5% and HMA_10%.

Figure 4 illustrates the representative load-displacement curves of the SLJ tests prepared with pristine HMA and HMA_10% for three different overlaps 12, 18.5 and 25 mm and the three adopted adhesive thicknesses: 0.5 mm shown in Figure 4 (a), 1.0 mm in Figure (b) and 1.5 in Figure (c). The three Figures show that the curves are very similar for all the joint configurations. In all the cases, the values of the maximum loads related to the joints prepared with HMA_10% are higher than the ones prepared with HMA. Although the sustained values are different (increasing with the overlap lengths), the trends of the pristine adhesive curves are very similar to each other as well as for the adhesive joints prepared with HMA_10%. The maximum loads for all the three different overlaps are not only increased but they are moved rightward in the diagram and then the loads decrease more slowly for the curves with a lower overlap. Furthermore, Figures 4 (a), (b) and (c) show that the increase of the adhesive thickness leads to lower loads and higher displacements. Figure 4 (a) displays a different trend for the curve related to the joint prepared with an overlap of 25 mm, a thickness of 0.5 mm and with HMA_10%. In this case, a large deformation of the substrate was observed by visual inspection that is shown in Figure 5.
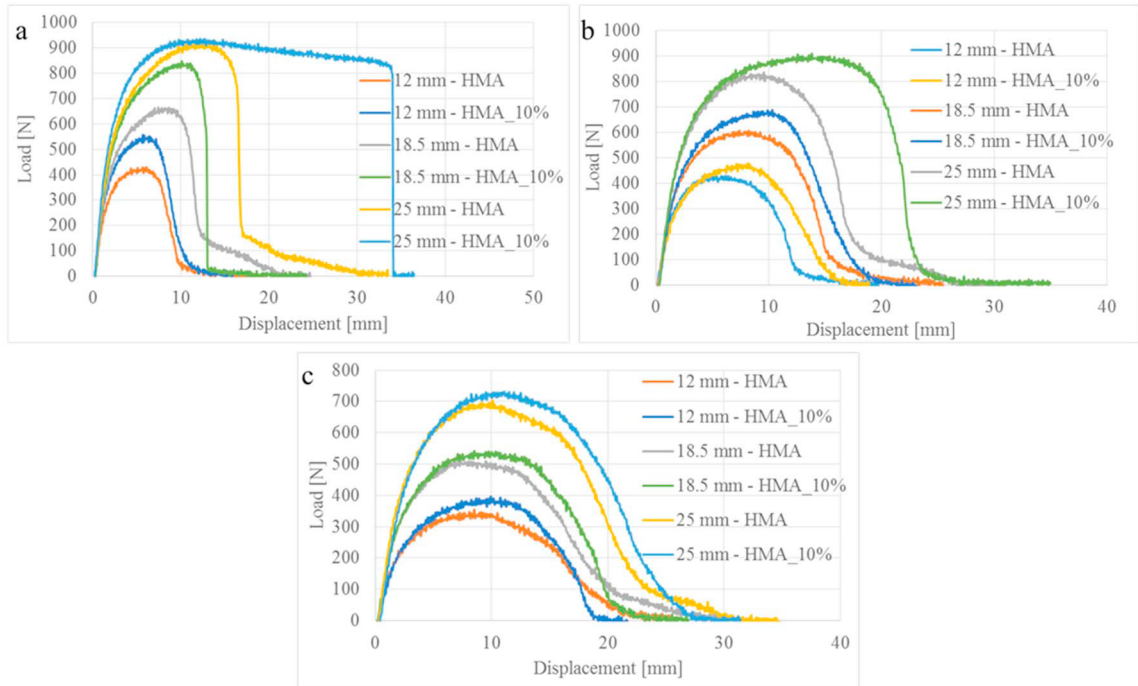
Fig. 4: Representative curves of SLJ tests for 12 mm, 18.5 and 25 overlaps and the three different adhesive thicknesses: (a) 0.5 mm, (b) 1.0 mm and (c) 1.5 mm

Figure 5 shows the fracture surfaces of the lap joints prepared with pristine HMA and HMA_10% respectively for the six different analyzed overlaps and thicknesses. As depicted in the previous section, Figure 2.17, the cohesive surfaces for the joints prepared with HMA_10% present a larger area than the ones prepared with HMA. Generally, the lower overlaps present a larger cohesive area compared to the bigger one. The SLJ specimens prepared with the overlaps of 12 and 18.5 mm and the thicknesses of 0.5 and 1.0 mm present a mostly cohesive zone while in the other ones, the adhesive failure mode is larger. The SLJ specimen prepared with a 0.5 mm thickness and 25 mm overlap presented a deformation of the substrate that led to an adhesive failure and also to a different trend of the curve, as seen in Figure 4 (a).
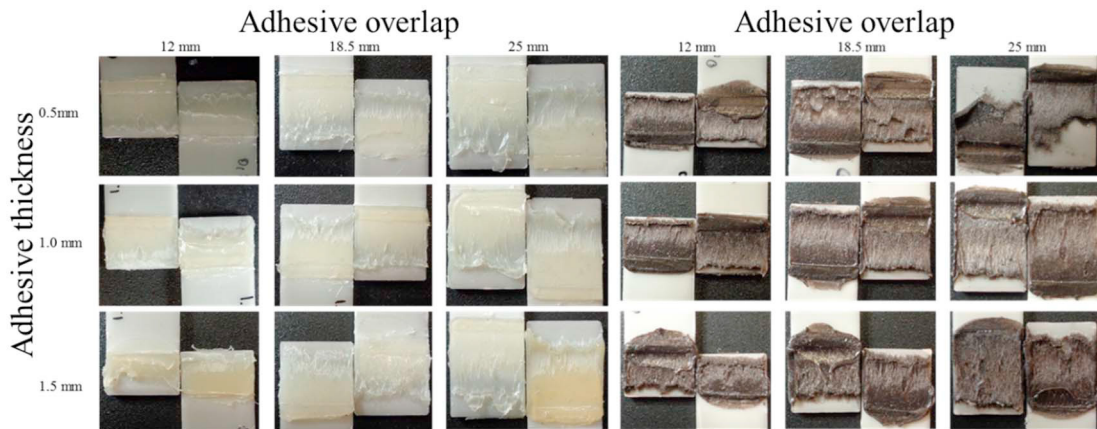

Fig. 5: Fracture surfaces of the SLJ prepared with HMA and HMA_10%

Figure 6 shows the effect of the adhesive thicknesses and overlaps on the maximum average adhesive load and strength for the SLJ prepared HMA and HMA_10%. As expected the maximum sustained load increases for larger overlaps decreases for thinner adhesive thicknesses. Figure 6 (b) shows that the trends of the maximum loads for the

adhesive joints prepared with HMA_10% are very similar to the joints prepared with HMA. Comparing the two diagrams, it is evident that the maximum sustained loads are larger for the case of HMA_10%.

It is noticeable, that the values of the maximum loads for the joints prepared with HMA and an overlap of 12 mm are closer compared to the ones prepared with HMA_10% and the same overlap. Furthermore, the increase of maximum load for the modified adhesive is more evident for the overlaps of 18.5 mm and 25 mm. The tendency lines in both Figures (a) and (b) show that the strengths are almost constant for a fixed thickness. The only one that shows a change of curvature is the tendency line of the SLJ prepared with HMA_10% and with a thickness of 0.5. The reason is due to the change in the failure mode. The values of the standard deviations are reported in the error bars of both Figures 2.18 and 2.19 and the scatter is very limited. For both cases, the values of the shear strengths for the shortest overlap are higher compared to the larger ones since the resistance areas are higher due to the fact that the central part of the overlap (reduced in this case) is a zone with low stress, see Boursier et al. (2018), Scattina et al. (2011).
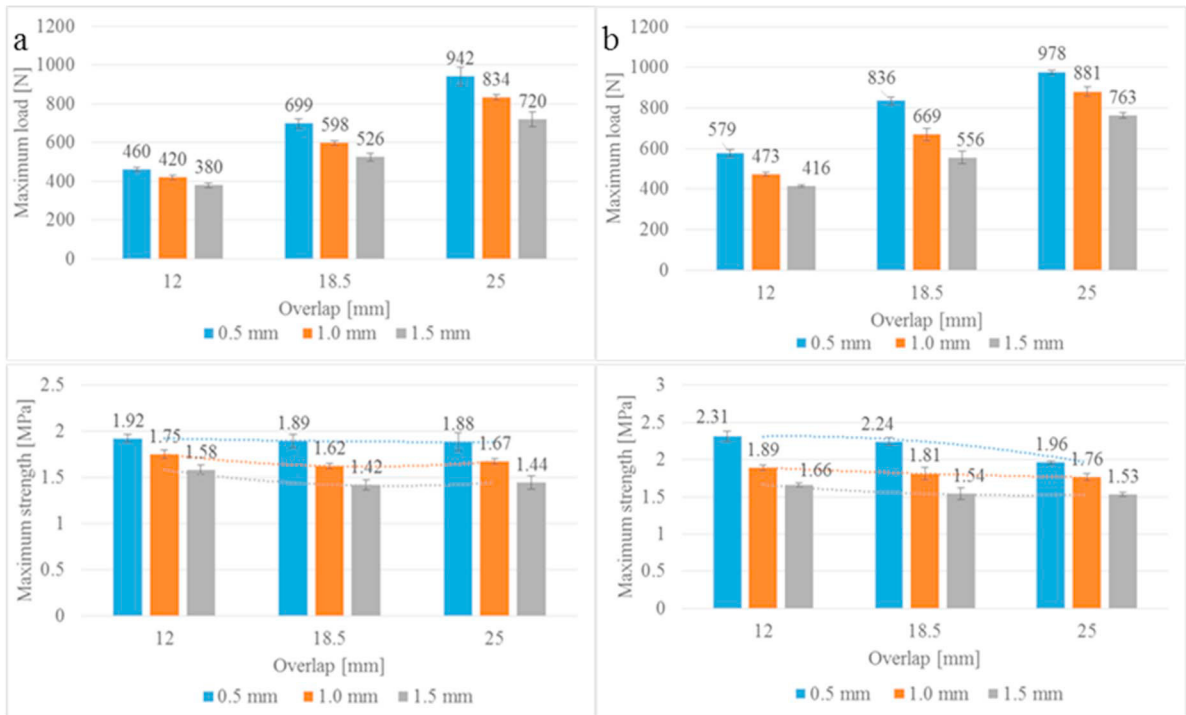

Fig. 6: Effect of the adhesive thicknesses and overlaps on the maximum load and strength for the pristine HMA (a) and HMA_10% (b).

Figure 7 reports the representative curves for the overlap lengths that leads to a failure of the substrates for joints prepared with the pristine HMA, Figure (a), and HMA_10%, Figure (b). The curves are at a fixed adhesive thickness, that is 1 mm. The curve related to the overlap of 25 mm has been also added to have a direct comparison with a curve where the failure was mainly cohesive. The SLJ specimens prepared with 31.5, 37 and 50 mm overlap lengths and an adhesive thickness of 1.0 mm, lead to substrates failure for both HMA and HMA_10%. These curves have been reported in order to show that these curves are very close to the tensile test made on PP substrates, see Koricho et al. (2016). The curves for both the cases of HMA and HMA_10% are very similar when substrates deformation occurs.
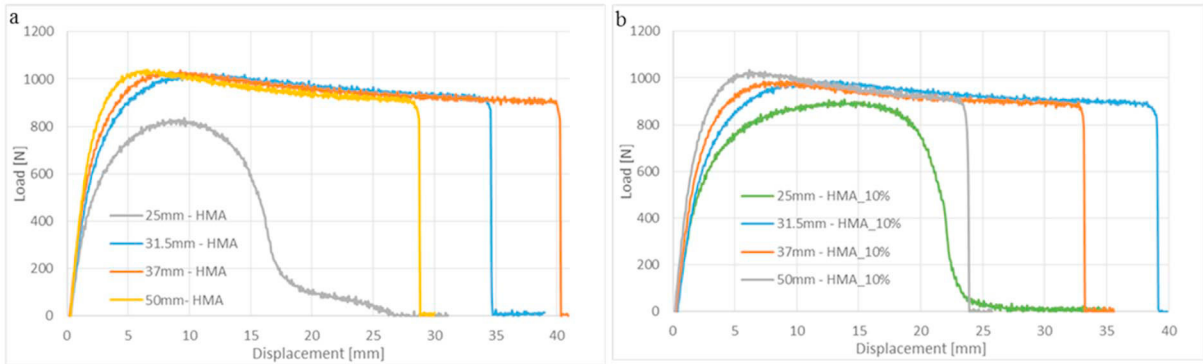
Fig. 7: Comparison of representative curves of adhesive joints prepared with 25, 31.5, 37 and 50 mm overlaps: (a) for HMA; (b) for HMA_10%

3.2. Separation tests

The sensitivity of nanomodified adhesives to electromagnetic fields have been widely studied by Ciardiello et al. (2019). The work studied the effects of current, power, frequency and shape of the electromagnetic field on the separation time of the joints. This study was carried out on the same masterbatch of the adhesives studied in this work. Based on that main results of Ciardiello et al. (2019), the separation tests were conducted by using all the parameters that minimize the separation time that is: highest frequency, highest power (and current) and a solenoidal coil that maximize the electromagnetic field in the center. Figure 8 summarizes the main results obtained by the separation tests. In particular, Figure 8 (a) reports the separation times that were obtained with the three different adhesive overlaps and thicknesses. Figure 8 (a) is separated into two parts because of the different scales related to the separation times. The main point of this figure is that the separation time does not change significantly with the overlap as shown by the bars on the left side of the figure and by the standard deviations reported by the error bars. On the other hand, the separation time is highly sensitive to the adhesive thickness. In fact, the separation time of the joints prepared with a thickness of 0.5 mm is 400% higher than the case with a 1.0 mm thickness. However, Ciardiello et al. (2019) explained that this is due to the higher interfacial strength of the adhesive joint with a thickness of 0.5 mm compared to the ones of 1.0 and 1.5 mm, as shown in the mechanical properties section. In fact, the analysis conducted with a thermal camera and reported in that study has shown that the substrate temperature of the joint prepared with a thickness of 0.5 mm before the separation was very high compared to 1.0 and 1.5 mm. This was connected to the small weight used for initiating the sliding of the lower substrate when the adhesive was melted. This behavior explains the higher separation time as well. Figure 8 (b) shows the results of the separation tests of adhesive joints prepared with the three adhesive compositions. As expected, the lowest separation times are related to the adhesive joints prepared with HMA_10%. Furthermore, HMA_10% present also the lowest standard deviation. This is related to the dispersion of the particles. In fact, HMA_3% and HMA_5% presented some areas with a lower presence of particles that need to be melted by conduction, as shown by Ciardiello et al (2019). Figure 8 (c) displays a representative separation surface of the SLJ after the dismounting operations. In all the analyzed cases, the separation was cohesive.
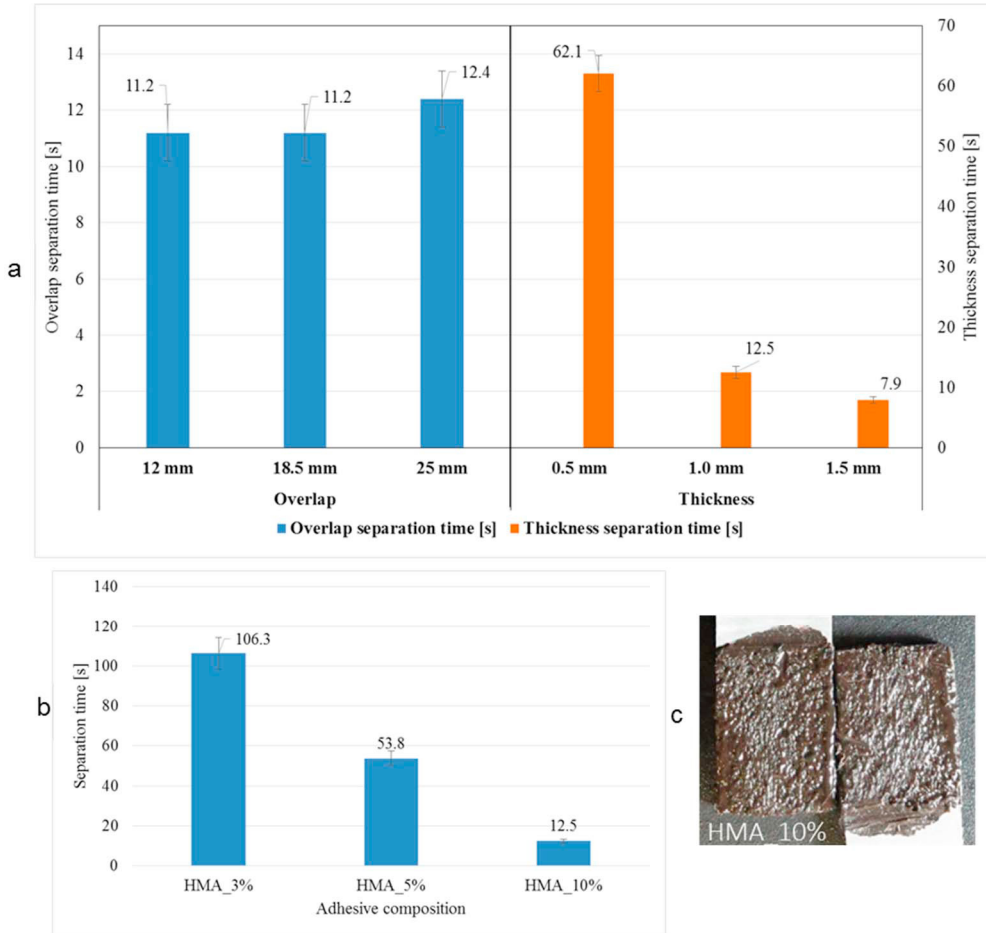
Fig. 8: (a) separation time for different overlaps and thicknesses; (b) separation time for different adhesive compositions; (c) representative separation surface after induction heating.

3.3. Scanning electron microscope analysis

A complete study of the particle distribution of iron oxide particles within this hot-melt adhesive mixed with the mixing method adopted in this work has been presented in Ciardiello et al. (2018) and Ciardiello et al. (2019). These studies were carried out on the same masterbatch and showed that the mixing method used in this work offers a uniform distribution of the particles however it is not able to completely separate the small nanoparticle aggregates that tend to form clusters with an average length of 0.78 μm. Although a comprehensive study of the microscopy analysis has been reported in the cited studies for all the three adhesive compositions, a representative SEM image has been reported in order to show the presence of the agglomerates and the distribution of the particles. Figure 9 shows the presence of these agglomerates fir HMA_10% that are represented by the whiter spots. However, the presence of the clusters was found also in HMA_3% and HMA_5% as shown in Ciardiello et al. (2019). Furthermore, the case of HMA_3% and HMA_5% displayed some areas where the presence of the particles was lower that led to a higher separation time as reported in the previous section.
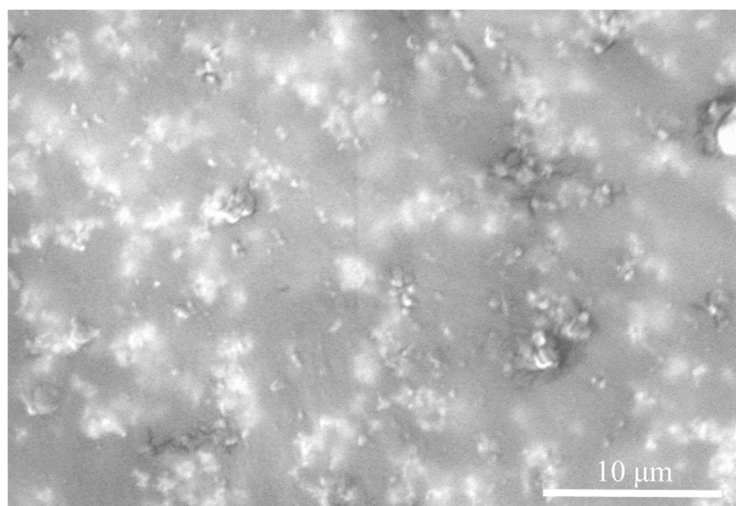
Fig. 9: Representative SEM image of HMA_10%

4. Conclusion

This paper presents a comprehensive study of the mechanical properties of reversible plastic joints. These joints can be dismounted by means of induction heating that is able to heat iron oxide particles embedded in the adhesive matrix. In particular, this work provided the mechanical behavior of adhesive single lap joints prepared with a pristine polyolefin adhesive and three different weight concentrations of iron oxide nanoparticles, 3%, 5% and 10%. Three different thicknesses and six overlaps were analyzed prepared with HMA and HMA_10% to study the mechanical behavior of adhesive joint in many configurations. Furthermore, the separation tests were carried out taking into account the results presented by Ciardiello et al. (2019) in order to minimize the separation time and evaluate the possibility to use this technique in manufacturing processes. The main outcomes of this work are summarized below.

- The mechanical properties of modified adhesives were evaluated with different configuration and compared with the pristine adhesive in order to understand whether this adhesive can be used for automotive application. As anticipated in the introduction of this work, the addition of nanoparticles can lead to a detrimental effect of the mechanical properties in some cases. However, all the analyzed cases present a higher value of the modified adhesive compared to the basic HMA both on the maximum load and the ductile behavior. The increase of the mean value of the modified adhesive over the pristine one is around 5% for the adhesive modified with 3% and 5% wt., while it is of 7% for HMA_10%. Mechanical results conducted on different overlaps and thicknesses showed that the mean maximum loads of the modified adhesive are higher of the pristine ones in all the cases. The increases are more evident for the joints prepared with an adhesive thickness of 0.5 mm where the increase of the modified adhesive over the pristine adhesive was around 20%. This increase is lower for the joint prepared with 1.0 mm thickness where the increase was around 10% higher and 7% for the joint prepared with a thickness of 1.5 mm.
- The separation tests reported in this work confirmed the results obtained by Ciardiello et al. (2019). This work shows that the separation time does not change significantly with the overlap. On the other hand, the separation time is highly affected by the adhesive thickness. The separation time of the joints prepared with a thickness of 0.5 mm is 400% higher than the case with a 1.0 mm thickness. However, this could be connected to the higher adhesive strength of the adhesive prepared in this configuration and to the low used weight to start the sliding when the adhesive melts. The separation tests conducted on adhesive joints prepared with HMA_3%, HMA_5% and HMA_10 showed that the lowest separation time is recorded for the joints prepared with HMA_10%.

- SEM analysis carried out on HMA_10% was reported despite a compressive study on the same masterbatch was presented in Ciardiello et al. (2019). This work confirmed that the particles tend to form small clusters that are uniformly distributed in the matrix.

References

Banea, M., 2019. Debonding on demand of adhesively bonded joints: a critical review. Reviews of Adhesion and Adhesives 7(1), 33-50.

Banea, M., da Silva, L., Carbas, R., 2015. Debonding on command of adhesive joints for the automotive industry. International Journal of Adhesion and Adhesive 59, 14–20.

Banea, M.D., da Silva, L.F.M., Campilho, R.D.S.G., 2013. An overview of the technologies for adhesive debonding on command. Annals of "Dunarea de Jos" University of Galati, Fascicle XII, Welding Equipment and Technology 24, 11-14.

Bayerl, T., Duhovic, M., Mitschang, P., Bhattacharyya, D., 2014. The heating of polymer composites by electromagnetic induction – A review. Composites: Part A 57, 27-40.

Belingardi, G., Brunella, V., Martorana B., Ciardiello, R., 2016. Thermoplastic adhesive for automotive applications, in "Adhesive – Application and properties". Rudawska, A. (Ed.). INTECH, Rijeka pp. 341.

Belingardi, G., Chiandussi, G., 2004. Stress flow in thin walled box beams obtained by adhesive bonding joining technology. International Journal of Adhesion and Adhesive 24, 423–439.

Boursier Niutta, C., Ciardiello, R., Belingardi, G., Scattina, A., 2018. Experimental and numerical analysis of a pristine and a nano-modified thermoplastic adhesive. PVP® Pressure Vessels & Piping Conference, Prague, Czech Republic, paper #84728.

Casalegno, V., Salvo, M., Rizzo, S., Goglio, L., Damiano, O., Ferraris, M., 2018. Joining of carbon fibre reinforced polymer to Al-Si alloy for space applications. International Journal of Adhesion and Adhesive 82, 146-152.

Chang, B., Shi, Y., Dong, S., 1999. Comparative studies on stresses in weld-bonded, spot-welded and adhesive-bonded joints. Journal of Materials Processing Technology 87, 230–236.

Ciardiello, R., Belingardi, G., Martorana, B., Brunella, V., 2018. Effect of accelerated ageing cycles on the physical and mechanical properties of a reversible thermoplastic adhesive. The Journal of Adhesion. In press: https://doi.org/10.1080/00218464.2018.1553714.

Ciardiello, R., Belingardi, G., Martorana, B., Brunella, V., 2019. Physical and mechanical properties of a reversible adhesive for automotive applications. International Journal of Adhesion and Adhesive 89, 117–128.

Ciardiello, R., Belingardi, G., Martorana, B., Fondacaro, D., Brunella, V., 2016. A study of physical and mechanical properties of a nanomodified thermoplastic adhesive in normal and accelerated ageing conditions. 17th European Conference on Composite Materials, Munich, Germany.

Ciardiello, R., Martorana, B., Lambertini, V. G., Brunella, V., 2017. Iron-based reversible adhesives: Effect of particles size on mechanical properties. Proceedings of the Institution of Mechanical Engineers, Part C: Journal of Mechanical Engineering Science 232(8), 1446–1455.

Ciardiello, R., Tridello, A., Brunella, V., Martorana, B., Paolino D.S., Belingardi, G., 2017. Impact response of adhesive reversible joints made of thermoplastic nanomodified adhesive. The Journal of Adhesion 94(12), 1051–1066.

Ciardiello, R., Tridello, A., Goglio, L., Belingardi, G., 2018. Experimental assessment of the dynamic behavior of polyolefin thermoplastic hot melt adhesive. PVP® Pressure Vessels & Piping Conference, Prague, Czech Republic, paper #84725.

Directive 2000/53/EC of the European Parliament on end-of life vehicles. 18 September 2000.

Directive 2005/64/EC of the European Parliament on the type-approval of motor vehicles with regard to their reusability, recyclability and recoverability. 26 October 2005.

Ghazanfari, M., Kashefi, M., Shams, S., Jaafari, M., 2016. Perspective of Fe₃O₄ Nanoparticles Role in Biomedical Applications. Biochemistry Research International 2016, 1-32.

Koricho, E., Verna, E., Belingardi, G., Martorana, B., Brunella, V., 2016. Parametric study of hot-melt adhesive under accelerated ageing for automotive applications. International Journal of Adhesion and Adhesive 68, 164–181.

Lu, Y., Broughton, J., Winfield, P., 2014. A review of innovations in disbonding techniques for repair and recycling of automotive vehicles. International Journal of Adhesion and Adhesive 59, 119–27.

Moskowitz, B.M., Frankel, R.B., Walton, S., Dickson, D.P., Wong, K.K., Douglas T, Mann, S., 1997. Determination of the preexponential frequency factor for superparamagnetic maghemite particles in magnetoferritin. Journal of Geophysical Research 102(97), 226-271.

Rudawska, A., 2010. Adhesive joint strength of hybrid assemblies: Titanium sheet-composites and aluminium sheet-composites—Experimental and numerical verification. International Journal of Adhesion and Adhesive 30(7), 574-582.

Rudawska, A., Worzakowska, M., Bociąga, E., Olewnik-Kruszkowska, E., 2019. Investigation of selected properties of adhesive compositions based on epoxy resins. International Journal of Adhesion and Adhesive 92, 23-36.

Scattina, A., Peroni, L., Peroni, M., Avalle, M., 2011. Numerical analysis of hybrid joining in car body applications. Journal of Adhesion Science and Technology 25, 2409-2433.

Severijns, C., Teixeira de Freitas, S., Poulis, J.A., 2017. Susceptor-assisted induction curing behaviour of a two component epoxy paste adhesive for aerospace applications. International Journal of Adhesion and Adhesive 75, 155-164.

Suwanwatana, W., Yarlagadda, S., Gillespie J.W., 2006. Hysteresis heating based induction bonding of thermoplastic composites. Composites Science and Technology 66, 1713–1723.

Vattathurvalappil, S.H., Haq, M., 2019. Thermomechanical characterization of Nano-Fe₃O₄ reinforced thermoplastic adhesives and single lap-joints. Composites Part B: Engineering 175. In press: Article number 107162 (https://doi.org/10.1016/j.compositesb.2019.107162).

Verna, E., Cannavaro, I., Brunella, V., Koricho, E. G., Belingardi, G., Roncato, D., Martorana, B., Lambertini, V., Alina Neamtu, V., Ciobanu, R., 2013. Adhesive joining technologies activated by electro-magnetic external trims. International Journal of Adhesion and Adhesive 46, 21–25.